Crystal Structure and Polymorphism of Antiferroelectric Mesogen, 4-[(*S*)-1-Methylheptyloxycarbonyl]phenyl 4′-Octyloxybiphenyl-4-carboxylate (MHPOBC)

Kayako HORI* and Kyoko ENDO
Department of Chemistry, Ochanomizu University, Otsuka, Bunkyo-ku, Tokyo 112
(Received August 6, 1992)

Single crystal X-ray analysis has been carried out for the title compound, $C_8H_{17}O$-⟨⟩-⟨⟩-COO-⟨⟩-COOCH-$(CH_3)C_6H_{13}$, which has antiferroelectric liquid crystalline phases. Crystal data; monoclinic, $P2_1$, $T=298$ K, $a=32.285(7)$, $b=5.520(2)$, $c=9.320(2)$ Å, $\beta=95.34(2)°$, $V=1653.7(7)$ Å^3, $Z=2$, $d_x=1.123$ g cm^{-3}. The crystal has a smectic-like layer structure composed of largely bent molecules; a chain of the chiral group is almost perpendicular (93°) to the core moiety. DSC and temperature dependence of powder X-ray diffraction patterns show that the crystal is a metastable phase, which transforms to a more stable crystalline phase with longer spacing of layer.

4- [(*S*)- 1- Methylheptyloxycarbonyl] 4′- octyloxybiphenyl-4-carboxylate (MHPOBC) has been widely studied as the first example exhibiting antiferroelectric liquid crystalline phases.[1] It has a phase sequence of cryst.–Sm*C_A–Sm*C_γ-Sm*C–Sm*C_α–Sm A–iso.[2] Here, Sm*C_A, Sm*C (originally denoted Sm*C_β) and Sm*C_γ are antiferroelectric, ordinary ferroelectric,[2] and ferrielectric phases,[1] respectively. Sm*C_α is assumed to be a helical biaxial Sm A.[3] In addition, another antiferroelectric phase, a supercooled Sm*I_A also appears on cooling.[2]

In order to elucidate the intermolecular interaction controlling this very complicated and interesting behavior, we have carried out single crystal X-ray analysis for this compound, since good correlation has been found between crystal structures and mesophase behavior for several series of chiral smectogenic biphenyl esters.[4] This paper describes the crystal structure and phase relation between crystalline polymorphs as well as between the crystal and liquid crystals.

Experimental

Powder diffraction patterns were obtained on a Rigaku RAD-RA diffractometer. DSC measurements were done on a Seiko SSC570 calorimeter.

Crystal Structure Analysis. Colorless long plate-like crystals were grown from an ethyl acetate-methanol solution.

Accurate cell parameters were determined by a least-squares fit for 15 reflections within the range, $40<2\theta<49°$, measured on a Rigaku AFC-4 diffractometer with Cu $K\alpha$ radiation ($\lambda=1.54184$ Å) monochromated by graphite. Crystal data; 4-[(*S*)-1-methylheptyloxycarbonyl]phenyl 4′-octyloxybiphenyl-4-carboxylate, $C_{36}H_{46}O_5$, $M_r=558.76$, monoclinic, $P2_1$, $T=298$ K, $a=32.285(7)$, $b=5.520(2)$, $c=9.320(2)$ Å, $\beta=95.34(2)°$, $V=1653.7(7)$ Å^3, $Z=2$, $d_x=1.123$ g cm^{-3}, $F(000)=604$, $\mu=5.08$ cm^{-1}.

Intensity data were measured on the diffractometer using a crystal of $0.5\times0.5\times0.02$ mm up to $2\theta=125°$. A 2θ–ω scan mode with scan width of $\omega=(1.0+0.15\tan\theta)°$ and scan rate of $4°(2\theta)$ min^{-1} was applied. Backgrounds were counted for 5 s at both ends of a scan. Three standard reflections were recorded after every 50 reflections. No significant intensity variations were observed. A total of 2970 reflections were collected, of which 1185 were treated as significant ($|F_o|>4\sigma(|F_o|)$). The data were corrected for Lorentz and polarization factors but not for absorption.

The structure was solved by applying the program MULTAN78[5] and refined by full-matrix least-squares using SHELX76.[6] The quantity minimized was $\Sigma w(|F_o|-|F_c|)^2$, where $w=(0.004|F_o|^2+\sigma(|F_o|)^2)^{-1}$. Atomic scattering factors were taken from the International Tables for X-Ray Crystallography.[7] In the course of refinement, several additional peaks of 0.5—0.7 eÅ^{-3} were found around both of the chains, whose atoms had remarkably large temperature factors. These peaks were included as disordered atoms in further refinement. All the non-hydrogen atoms except for the disordered atoms were refined anisotropically. Only 12 hydrogen atoms found in the difference Fourier maps were included in the refinements, due to the limited number of reflections. Max. Δ/σ and max. $\Delta\rho$ in the final difference map were 0.21 and 0.29 eÅ^{-3}, respectively. Final R and R_w were 0.125 and 0.137, respectively. The large R value is due to the poor crystallinity in spite of repeated attempts of crystallization and the fact that the chains are highly disordered. Computations were carried out on an IBM 4381-R24 computer at the Information Processing Center of Ochanomizu University. Final atomic coordinates are shown in Table 1.[8]

Results and Discussion

Molecular Conformation. Figure 1 shows a molecular structure with a numbering scheme. All the bond lengths and angles are compatible with those of other mesogens.[4] The most striking feature, however, is that the chain of the chiral group is almost perpendicular to the core moiety, in contrast to all other mesogens determined previously. The bent angle is estimated to be 93°. Table 2 shows the torsion angles of paraffin chains. The chain of the chiral group is highly disordered with twisted conformations, while the normal paraffin chain has relatively extended conformations, which is also disordered at the terminal moiety. Biphenyl moiety is almost coplanar with the dihedral angle of 4.3°.

Crystal Packing. Figure 2 shows a crystal pack-

Table 1. Final Atomic Coordinates Multiplied by 10^4 and Equivalent Isotropic Thermal Parameters (B_{eq}) for MHPOBC

Atom	x	y	z	B_{eq} [a]/Å^2
O(1)	6196(4)	4517(46)	673(14)	8.2
O(2)	3319(5)	1759(50)	4799(15)	8.5
O(3)	3468(4)	5055	5999(21)	8.8
O(4)	1788(7)	3535(61)	9166(24)	14.1
O(5)	1688(5)	6840(57)	7972(16)	10.5
C(1)	5826(4)	4484(47)	1124(22)	8.2
C(2)	5710(5)	6259(43)	2077(17)	6.7
C(3)	5337(6)	6051(56)	2703(23)	12.0
C(4)	5066(4)	4141(45)	2359(13)	4.3
C(5)	5177(5)	2442(46)	1377(20)	7.6
C(6)	5562(6)	2522(45)	821(22)	9.8
C(7)	4671(4)	4046(47)	3101(15)	4.3
C(8)	4587(5)	5769(50)	4126(18)	9.4
C(9)	4214(5)	5683(49)	4757(17)	6.5
C(10)	3937(5)	3785(50)	4441(18)	5.8
C(11)	4024(5)	2087(53)	3411(23)	8.8
C(12)	4383(5)	2251(52)	2690(19)	7.6
C(13)	3571(12)	3394(74)	4986(39)	11.7
C(14)	3098(5)	5314(51)	6584(18)	6.5
C(15)	3013(6)	3444(48)	7516(22)	8.1
C(16)	2619(6)	3385(52)	8045(19)	8.6
C(17)	2325(8)	5221(54)	7758(25)	9.1
C(18)	2436(5)	7147(49)	6900(23)	7.9
C(19)	2826(5)	7257(48)	6372(22)	8.7
C(20)	1936(8)	4864(83)	8369(40)	10.9
C(21)	6344(6)	2859(48)	−348(16)	5.3
C(22)	6788(5)	3151(62)	−728(21)	7.6
C(23)	6945(7)	1128(67)	−1503(24)	9.4
C(24)	7376(7)	1689(54)	−1845(26)	8.2
C(25)	7590(11)	−459(91)	−2626(40)	15.4
C(26)	8012(13)	8(79)	−3074(37)	14.2
C(27)	8244(24)	−2886(110)	−3307(80)	13.7(26)
C(27′)	8148(36)	−1995(150)	−3162(94)	18.2(41)
C(28)	7988(16)	−3441(120)	−4204(55)	9.9(14)
C(28′)	8364(18)	−3490(160)	−4612(63)	13.8(20)
C(31)	1249(10)	7197(87)	8334(44)	16.5
C(32)	1029(9)	8630(100)	7110(42)	25.2
C(33)	868(12)	6643(110)	5710(36)	22.7
C(34)	494(18)	7980(170)	4879(74)	15.4(25)
C(34′)	693(21)	9164(120)	4499(70)	14.0(22)
C(35)	535(26)	7654(190)	3627(79)	13.7(24)
C(35′)	624(27)	6253(150)	3658(81)	14.5(29)
C(36)	195(38)	6831(210)	2424(120)	23.7(63)
C(36′)	389(31)	6490(240)	2612(110)	18.4(34)
C(37)	83(22)	8454(180)	1643(72)	15.4(22)
C(37′)	353(33)	3712(250)	2574(130)	24.9(43)
C(38)	1297(14)	8342(110)	9851(42)	21.6

a) $B_{eq}=(8\pi^2/3)\sum_i\sum_j U_{ij}\,\boldsymbol{a}_i\cdot\boldsymbol{a}_j$. b) Occupation factors of C(27), C(28), C(34)–C(37), and their counterparts were fixed to be 0.5. Isotropic temperature factors are shown for these atoms.

ing mode viewed along the b axis. In spite of the largely bent shape of the molecule, the crystal has a smectic-like layer structure. Interfaces of the layers are parallel to the (100) plane. Within a layer, a moiety except for the bent chain of each molecule takes a parallel arrangement, contributing to a large overlapping of molecules within a layer. A tilt angle is estimated to be 30°. The bent chains face each other between the neighboring layers.

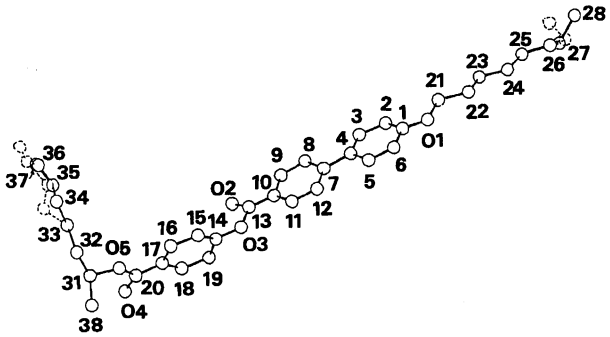

Fig. 1. Molecular conformation with a numbering scheme. Disordered atoms are shown by broken lines.

Table 2. Torsion Angles (τ) of Paraffin Chains

	τ/°	τ/° [a]
O(1)–C(21)–C(22)–C(23)	−167	
C(21)–C(22)–C(23)–C(24)	−178	
C(22)–C(23)–C(24)–C(25)	−177	
C(23)–C(24)–C(25)–C(26)	−177	
C(24)–C(25)–C(26)–C(27)	−160	−158
C(25)–C(26)–C(27)–C(28)	−61	−126
O(5)–C(31)–C(32)–C(33)	−82	
C(31)–C(32)–C(33)–C(34)	−155	−173
C(32)–C(33)–C(34)–C(35)	−140	−179
C(33)–C(34)–C(35)–C(36)	−133	−163
C(34)–C(35)–C(36)–C(37)	−106	167

a) Angles for another conformer.

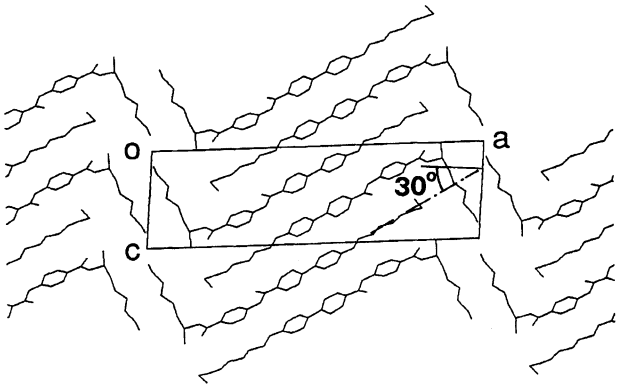

Fig. 2. Crystal structure viewed along the b axis. Only one of the disordered chains is denoted for clarity.

Figure 3 shows the crystal structure viewed along the c axis. Relatively short O–O distances are shown. Here, van der Waals contacts of oxygen atoms are avoided in a parallel arrangement of the molecules, because the ester group moiety is narrower than the bulges of the phenyl rings. Ester groups are arranged in infinite chains of relatively close head-to-tail arrangements along the b axis. The directions of the head-to-tail arrangements for the two ester groups in a molecule are the same

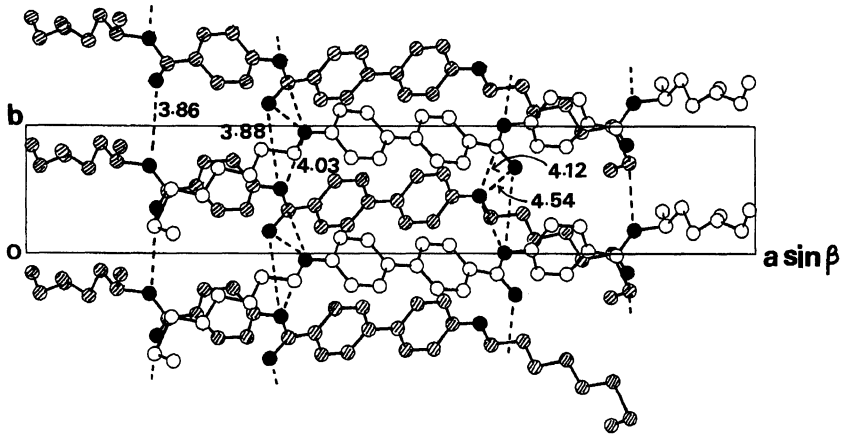

Fig. 3. Crystal structure viewed along the c axis. Only one of the disordered chains is denoted for clarity. Oxygen atoms are denoted by black circles. Molecules at the back are shadowed. Numerical values are O–O distances (Å).

along the b axis. All the molecules, related by a 2-fold screw axis along the b axis, have the same direction of the head-to-tail arrangements of esters concerning the b axis. The direction of a dipole moment associated with an ester group lies across the major axis of the molecule.[9] Thus, the components of dipole moments along the b axis are not zero but added, making each layer highly polar. Since the polar layers are stacked in a parallel way, the whole crystal is also highly polar.

Thermal Behavior. Figure 4a shows a DSC diagram obtained for the single crystals prepared in this study. The curve is essentially the same as that obtained previously for the powder specimen.[10] At the first endothermic peak, the crystals (I) transform to another crystalline phase (II). At the exothermic peak just after the second endothermic peak about 70°C, the crystal II transforms irreversibly to a more stable crystalline phase (III). This is confirmed by the second run, in which the sample heated to 75°C and then cooled to room temperature was reheated. It shows only an endothermic peak at 80°C, as shown in Fig. 4b. Thus the crystals I and II are in metastable states. A Gibbs energy-temperature diagram is schematically shown in the figure. Considering the fact that supercooled Sm*C_A–Sm*I_A transition was observed at 64.5°C on cooling,[10] which is also shown in the diagram, it is reasonably derived that both crystals (II and III) transform to the same phase, i.e. Sm*C_A. This is also consistent with the fact that the entropy changes at 70 and 80°C are of similar order, although the former is not accurately estimated due to the following exothermic peak. It is concluded that the transition from the crystal II to Sm*C_A at 70°C triggers an exothermic transition to the more stable crystal III, which is shown by a solid arrow in the diagram. Then the crystal III transforms to Sm*C_A at 80°C.

Figure 5 shows the temperature dependence of powder X-ray diffraction patterns. The pattern at room temperature (Fig. 5a) shows a long spacing of 31.8 Å,

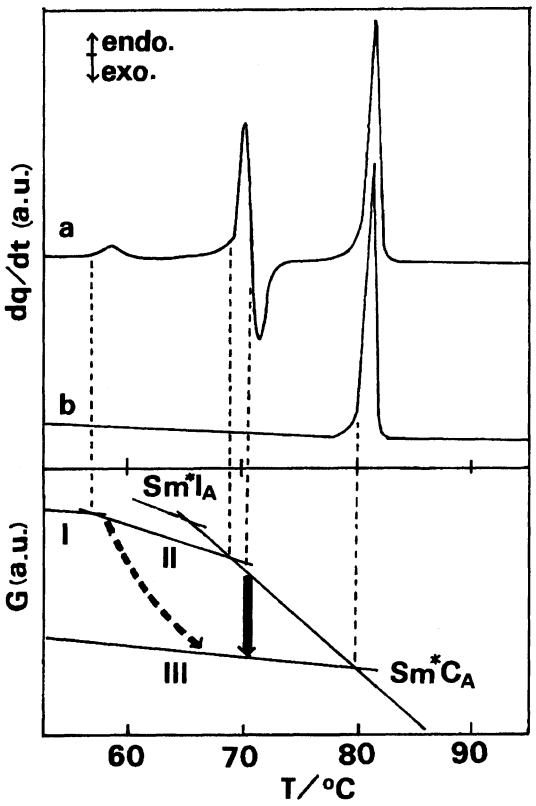

Fig. 4. DSC curves with scanning rate of 1 K min^{-1} for a) single crystals prepared in this study and b) the specimen previously heated to 75°C and then cooled to room temperature. Gibbs energy-temperature diagram is shown in the lower part of the figure. Solid and broken arrows denote stabilization process in rapid and slow heating, respectively.

which agrees with the layer thickness, $a \cdot \sin\beta = 32.14$ Å, within the experimental error. This pattern remains until the temperature reaches to 58°C, the first endothermic point (Fig. 4a). Then the pattern changes gradually in the temperature range of 58 to 70°C. The peaks of 31.8, 16.1, and 10.7 Å (regarded as the first, second, and

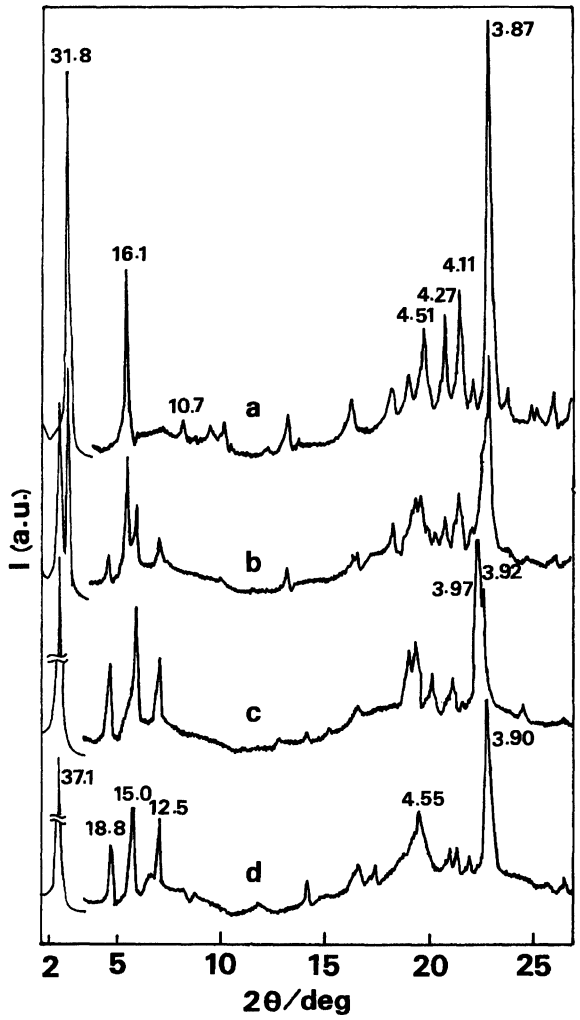

Fig. 5. Powder X-ray diffraction patterns. Peaks at 2—3° are multiplied by 1/10. a) virgin sample at room temperature. b) at 62°C. c) at 75°C. d) specimen previously heated to 75°C and then cooled to room temperature. The *d*-values of main peaks are shown in Å.

third diffraction of the layer) become weaker to vanish, while the peaks of 37.1, 18.8, 15.0, and 12.5 Å grow up. A pattern at the higher angles is also changed. Figure 5b shows an intermediate state of the change. The completely changed pattern from that at room temperature remains constant within the range from 70°C to 80°C, just below the cryst-Sm*C_A transition. Figure 5c shows the pattern at 75°C.

On the other hand, some drastic change would be expected around 70°C from the DSC result, which shows a large endothermic peak followed by an exothermic one at 70°C (Fig. 4a). This is, however, interpreted as follows. In the X-ray diffraction study, the temperature was kept constant for about 30 min for each scan. This procedure has an annealing effect, causing a gradual stabilization from the crystal I to the crystal III at lower temperature than that in the more rapid scan of DSC. This behavior is schematically shown by a broken arrow in Fig. 4.

The peaks, 37.1, 18.8, and 12.5 Å are regarded to be the first, second, and third diffraction of the layer. Therefore, the layer thickness becomes longer during the stabilization process. Figure 5d shows a pattern at room temperature for the specimen previously heated to 75°C. The long spacing is the same as that in the Fig. 5c while the pattern at higher angles is slightly but distinctly changed. Therefore, the structure with the layer thickness of 37 Å is retained at room temperature, while further rearrangements occur in the lateral packing of molecules during the cooling process.

It is concluded that the present crystal structure, thermodynamically metastable but frequently encountered, has a largely overlapped smectic-like layer structure with additive ester-ester interactions, which make each layer highly polar. The high polarity of the layer would be responsible for antiferroelectricity in the liquid crystal phase, where the structure would be stabilized by an alternate arrangement of the highly polar layers.

The authors express their sincere thanks to Professor Hideo Takezoe of Tokyo Institute of Technology for supplying the sample and Professor Yuji Ohashi of the Institute for measuring the reflection data on a single crystal. This work was partially supported by a Grant-in-Aid for Scientific Research No. 04640433 from the Ministry of Education, Science and Culture.

References

1) H. Takezoe, J. Lee, Y. Ouchi, and A. Fukuda, *Mol. Cryst. Liq. Cryst.*, **202**, 85 (1991), and references cited therein.

2) A. D. L. Chandani, E. Gorecka, Y. Ouchi, H. Takezoe, and A. Fukuda, *Jpn. J. Appl. Phys.*, **28**, L1265 (1989).

3) J. Lee, Y. Ouchi, H. Takezoe, A. Fukuda, and J. Watanabe, *J. Phys. Condens. Matter*, **2**, SA271(Proc. 1st Liq. Matter Conf., Lyon, 1990)(1990).

4) K. Hori and Y. Ohashi, *J. Mater. Chem.*, **1**, 667 (1991), and references cited therein.

5) P. Main, S. E. Hull, L. Lessinger, G. Germain, J.-P. Declercq, and M. M. Woolfson, "MULTAN78. A System of Computer Programs for the Automatic Solution of Crystal Structures from X-Ray Diffraction Data," Univ. of York, England and Louvain, Belgium (1978).

6) G. M. Sheldrick, "SHELX76, Program for Crystal Structure Determination," Umiversity of Cambridge, England (1976).

7) "International Tables for X-Ray Crystallography," Kynoch Press, Birmingham (1974), Vol. IV.

8) The table for the bond lengths and angles, the table for the anisotropic temperature factors for non-hydrogen atoms, the table for atomic parameters for hydrogen atoms and the $F_o - F_c$ list are deposited as Document No. 9054 at the Office of the Editor of Bull. Chem. Soc. Jpn.

9) G. W. Gray, "Molecular Structure and the Properties of Liquid Crystals," Academic Press, New York (1962), pp.

166.
10) A. D. L. Chandani, Y. Ouchi, H. Takezoe, A. Fukuda, K. Terashima, K. Furukawa, and A. Kishi, *Jpn. J. Appl. Phys.*, **28**, L1261 (1989).